

Numerical Calculations of the Density
and Temperature Variations in Cylindrical
Plasmas Preionized by UV-Radiation

M. Keilhacker

IPP 1/106

Mai 1970

INSTITUT FÜR PLASMAPHYSIK
GARCHING BEI MÜNCHEN

INSTITUT FÜR PLASMAPHYSIK

GARCHING BEI MÜNCHEN

Numerical Calculations of the Density and Temperature Variations in Cylindrical Plasmas Preionized by UV-Radiation

M. Keilhacker

IPP 1/106

Mai 1970

Die nachstehende Arbeit wurde im Rahmen des Vertrages zwischen dem Institut für Plasmaphysik GmbH und der Europäischen Atomgemeinschaft über die Zusammenarbeit auf dem Gebiete der Plasmaphysik durchgeführt.

(In English)

May 1970

Abstract

To get a picture of the time evolution of density, electron temperature, and ion temperature in cylindrical plasmas preionized by UV radiation, the relevant set of coupled differential equations is solved numerically. The model takes into account energy equipartitioning between electrons and the initially cold ions, radial ambipolar diffusion and heat conduction, and collisional ionization, excitation and recombination. As an example numerical results are presented for boundary conditions resembling those of the UV preionization of hydrogen and argon in a large diameter ($2R = 40$ cm) theta pinch. These show that the characteristic times for radial ambipolar diffusion and heat conduction can be made large relative to the energy equipartition time by superposing an axial magnetic field of the order of 100 gauss. The energy losses due to collisions with the neutral gas reduce the equilibration temperature by roughly 10 per cent.

I. Statement of the problem

One of the various possibilities of preionizing a plasma is by means of photoionization. The main drawback to this method of preionization lies in the difficulty of producing a light source that emits a sufficiently strong flux of photons in the relevant wavelength range ($\lambda \leq 800 \text{ \AA}$ for photoionization of H_2). Recently Hofmann/1/ and Keilhacker, Pecorella, and Vlases /2,3,4,5/ have developed a light source (in essence a z-pinch discharge in xenon; for details see /4,5/) that allows effective preionization of hydrogen and the noble gases. For example, in a 150 cm long test chamber with one of these light sources at each end the degree of ionization attainable in the median plane ranges, at a filling pressure of 1 mtorr, from 20 % in H_2 to 60 % in xenon /2,3,4,5/. The initial plasma thus produced ($n_e = 10^{12} - 5 \times 10^{13} \text{ cm}^{-3}$, $T_e = 1 - 2 \text{ eV}$ /4,5/) is quiescent, relatively homogeneous, and free of currents and impurities. Furthermore, the preionization works very well at lower filling pressures where other methods fail and, as far as photoionizing reactions are concerned, is independent of applied magnetic fields.

Preionization by means of photoionization therefore has many potential advantages and has successfully been used in collisionless shock wave experiments /6,7/, in which attainment of a uniform, current-free initial plasma presents a major problem.

This report deals with a model that describes the various processes taking place in a partially ionized plasma produced by photoionization. Numerical solution of the relevant set of coupled differential equations then allows us to follow the time development of density and temperature in such an initial plasma for realistic boundary conditions. It is thus possible to predict under what conditions (initial pressure, amplitude of applied magnetic field, etc.) and at what instant during the decay the parameters of the initial plasma are best suited to a particular experiment.

II. The equations used to describe the plasma

The model used is adapted to the general nature of plasmas produced by photoionization and to the special experimental conditions of the light source described in /4/ and /5/. Since the pulse of ultraviolet radiation emitted by the light source is short compared with the decay time of the photoionized plasma, the model starts when the build-up of plasma by photoionization has stopped, i.e. the equations contain no term describing photoionization. The model assumes an infinitely long plasma cylinder of radius R with a rectangular distribution of densities and temperatures at time $t = 0$.

One of the general features of photoionization is that only the electrons gain energy directly from the photoionizing radiation, while the ions are only heated by energy transfer from the electrons via collisions. The main question therefore is how the energy equipartition time compares with the particle and energy loss times. Another point of interest is how strong an axial magnetic field has to be in order to reduce considerably the losses due to ambipolar diffusion and radial heat conduction. The model therefore includes the processes of energy equipartitioning between electrons and ions, volume recombination, and ambipolar diffusion and heat conduction to the walls. Furthermore, in order to accommodate the fact that the plasma is only partially ionized, the effects of collisional excitation and ionization are included. Consideration of these two processes together with the effect of volume recombination distinguishes this model from an earlier one described in /4/ and /5/.

The problem is described by a continuity equation for electrons, an energy equation for electrons and ions respectively, and a macroscopic velocity given by the ambipolar diffusion approximation. These equations are:

$$\frac{\partial n_e}{\partial t} = -v_r \frac{\partial n_e}{\partial r} - n_e \frac{1}{r} \frac{\partial}{\partial r} (r v_r) + n_e n_n S - n_e^2 Q \quad (1)$$

$$\begin{aligned} \frac{\partial (k T_e)}{\partial t} = & -v_r \frac{\partial (k T_e)}{\partial r} - \frac{2}{3} (k T_e) \frac{1}{r} \frac{\partial}{\partial r} (r v_r) + \\ & + \frac{2}{3} \frac{1}{n_e} \frac{1}{r} \frac{\partial}{\partial r} (r \chi_e \frac{\partial T_e}{\partial r}) - \frac{1}{t_{eq}} (k T_e - k T_i) - \\ & - n_o S \left(\frac{2}{3} E_\infty + k T_e \right) - \frac{2}{3} n_o \sum_i P_i E_i \end{aligned} \quad (2)$$

$$\begin{aligned} \frac{\partial (k T_i)}{\partial t} = & -v_r \frac{\partial (k T_i)}{\partial r} - \frac{2}{3} (k T_i) \frac{1}{r} \frac{\partial}{\partial r} (r v_r) + \\ & + \frac{2}{3} \frac{1}{n_e} \frac{1}{r} \frac{\partial}{\partial r} (r \chi_i \frac{\partial T_i}{\partial r}) + \frac{1}{t_{eq}} (k T_e - k T_i) \end{aligned} \quad (3)$$

$$n_e v_r = -D_a \frac{\partial n_e}{\partial r}, \quad (4)$$

The boundary conditions for each of the equations are:

$$\frac{\partial A}{\partial r} = 0 \quad \text{for} \quad r = 0$$

$$A = A_R \quad \text{for} \quad r = R$$

$$A = A(0) \quad \text{for} \quad t = 0$$

where A stands for n_e , T_e , and T_i respectively.

P, S, and Q in Eqs. (1) and (2) are the rate coefficients for collisional excitation, ionization and recombination respectively, while E and E_∞ are the relevant excitation and ionization energies. The rate coefficients are calculated using relevant

cross-sections and folding them with a Maxwellian electron distribution of temperature T_e . Details about the cross-sections used are given in part III.

The neutral particle density follows from

$$n_n(r,t) = n_n(0) - n_e(r,t). \quad (5)$$

For the ambipolar diffusion coefficient D_a in a magnetic field the following expression⁺ is used (see, for example, /8/)

$$D_a = \frac{\frac{k T_i}{m_i} (1 + \frac{T_e}{T_n}) t_{cn}}{1 + \omega_e \omega_i t_{cn}^2}. \quad (6)$$

For the coefficients of heat conduction by electrons and ions, χ_e and χ_i , the following formulas /9/ for a fully ionized plasma are used (the corrections for the neutral gas component being negligible for our conditions):

$$\chi_e = 1.34 \frac{k}{m_e} n_e (k T_e) \frac{t_{ce}}{1 + 0.55 \omega_e^2 t_{ce}^2} \quad (7)$$

$$\chi_i = \frac{6.25}{\psi} \frac{k}{m_i} n_e (k T_i) \frac{t_{ci}}{1 + \frac{6.25}{\psi^2} \omega_i^2 t_{ci}^2} \quad (8)$$

where

$$\psi = 1.41 + 7.5 \left(\frac{m_e}{m_i} \right)^{1/2} \left(\frac{T_i}{T_e} \right)^{3/2}.$$

⁺) All formulas in c.g.s. units.

$\omega_{e,i} = \frac{e B_0}{m_{e,i} c}$ is the cyclotron frequency for electrons and ions, T_n the neutral gas temperature, and t_{cn} the collision time between electrons and neutrals (in a hydrogen gas $(t_{cn})^{-1} = 5.93 \times 10^9 \cdot p(\text{torr}) / 10$).

t_{ce} and t_{ci} are the self-collision times for electrons and ions respectively, and t_{eq} is the time for energy equipartitioning between electrons and ions. For these times, which are defined and calculated in /11/, the following formulas hold:

$$\begin{aligned}
 t_{ce} &= 1.7 \times 10^{23} \frac{(k T_e)^{3/2}}{n_e \ln \Lambda} \\
 t_{ci} &= \left(\frac{m_i}{m_e} \right)^{1/2} t_{ce} \\
 t_{eq} &= 0.516 \frac{m_i}{m_e} t_{ce} .
 \end{aligned}
 \tag{9}$$

The coefficients for radial ambipolar diffusion and heat conduction depend on the amplitude B_0 of an axial magnetic field. This dependence is of the form

$$D_a, \chi_e, \chi_i \sim \frac{1}{1 + C B_0^2} \quad C = \text{numerical factor}$$

Solving the inequality $C B_0^2 \gg 1$ for B_0 tells us how large a magnetic field has to be in order to have a noticeable effect on the diffusion coefficients.

In the case of ambipolar diffusion we find from eq. (6) for the necessary magnetic field

$$(B_0)_{\text{ambipol. diff.}} \geq 15 \sqrt{A} p \quad (10)$$

A = atomic weight

p = pressure in mtorr.

For 1 mtorr hydrogen this amounts to 15 gauss, for 1 mtorr argon to about 90 gauss.

Similarly, one gets from eq. (7) for the heat conduction by electrons (the heat conduction by ions is about $(m_i/m_e)^{1/2}$ times smaller for $T_e = T_i$)

$$(B_0)_{\text{heat cond.}} \geq 2.2 \times 10^{-13} \frac{n_e \ln \Lambda}{T_e^{3/2}} \quad (11)$$

T_e in eV.

For $n_e = 1 \times 10^{13} \text{ cm}^{-3}$ and $T_e = 1 \text{ eV}$, which are typical values for UV preionization, this yields a field of about 20 gauss. Thus, rather small magnetic fields of the order of 100 gauss should be sufficient to reduce ambipolar diffusion and heat conduction considerably.

III. Numerical results for some typical cases

We now discuss some typical numerical results for boundary conditions resembling those of the UV radiation preionization /4,5/ as applied to a large diameter ($2R = 40$ cm) collisionless shock wave experiment /12/. The initial values used for these calculations are summarized in Table 1.

The electron density at $t = 0$ was assumed to be $n_e(o) = 1 \times 10^{13} \text{ cm}^{-3}$ at a filling pressure of 1 mtorr H_2 or Ar (degree of ionization $\alpha \approx 30\%$) and $n_e(o) = 1$ or $5 \times 10^{13} \text{ cm}^{-3}$ at 10 mtorr ($\alpha \approx 3$ or 15%). The initial electron and ion temperatures, $T_e(0)$ and $T_i(0)$, were set equal to 2.0 eV and 0.1 eV respectively, while the neutral gas temperature T_n which enters into the calculation of D_a was kept at 0.026 eV ($\equiv 300^\circ \text{ K}$) throughout the calculations. The density and temperature at the plasma boundary were assumed to be $n_R = 1 \times 10^{11} \text{ cm}^{-3}$ and $T_{eR} = T_{iR} = T_R = 0.1$ eV. Varying n_R between 1×10^{10} and $1 \times 10^{12} \text{ cm}^{-3}$ and T_R between 0.025 and 0.4 eV did not noticeably change the results, except near the boundary. In the case of hydrogen, the plasma was assumed to be composed of electrons and H_2^+ ions (for H_2^+ ions energy equipartitioning would be a factor 2 slower); in the case of argon, of electrons and Ar^+ ions.

The rate coefficients appearing in eqs. (1) and (2) were taken from the following references. The rate coefficient for collisional recombination, Q , was calculated as a function of n_e and T_e by interpolating tabulated values of reference /13/. The rate coefficient for collisional ionization, S , was calculated using an empirical formula for ionization cross-sections proposed in reference /14/. This formula is asymptotically correct only for low densities, as lowering of the ionization potential and collision limit are not taken into account. Nevertheless it approximates all experimentally determined cross-section curves within the experimental error /14/.

The rate coefficients for collisional excitation, P_i , are not well known. Therefore the last term in eq. (2) that describes the cooling of electrons due to excitational collisions with

neutral atoms or molecules was omitted in most of the calculations. In order to get a feeling about the significance of this term on the electron temperature some of the hydrogen calculations were carried out both with and without this term (c.f. Figure 7). In this case the rate coefficients of reference /15/ were used.

Typical results of the numerical calculations are plotted in Figures 1 to 8.

Figures 1 to 6 show the time and space evolutions of the electron density n_e (dashed lines), electron temperature T_e (solid lines), and ion temperature T_i (solid lines) in a plasma described by eqs. (1) to (9) for the boundary conditions listed in Table 1. The numbers in brackets are the time in microseconds. As the energy equipartition time is proportional to the ions mass and inversely proportional to the density (c.f. eq.(9)) the time scales in Figures 1 to 6 are quite different. In the case of hydrogen the time for energy equipartition between electrons at 2 eV and ions at 0.1 eV is a few μsec at $n_e = 1 \times 10^{13} \text{cm}^{-3}$ and less than 1 μsec at $n_e = 5 \times 10^{13} \text{cm}^{-3}$, in the case of argon the corresponding times are about 300 μsec and 60 μsec respectively.

For the large diameter tube considered here the characteristic times for radial ambipolar diffusion and heat conduction are relatively long (they scale as R^2). During times of the order of the respective energy equipartition time the decay of density is almost negligible (except for the case of 1 mtorr H_2 with no axial magnetic field, shown in Figure 1a). In the case of hydrogen (Figures 1 to 3) the radial heat conduction losses are also small. In the case of argon (Figures 4 to 6), however, where the equipartition times are long, the heat conduction losses are substantial if no axial magnetic field is present. They can be reduced to a negligible value by superposition of an axial magnetic field of the order of 100 gauss (c.f. eq.(11)). The fact that even with magnetic field (Figures 4b,5b,6b) the equilibration temperature $T_{e,i}$ is somewhat smaller than it

should be without any losses (namely $(T_e(o)+T_i(o)) / 2 = 1,05$ eV) is due to the electrons losing energy in ionizing collisions with the neutral background. Due to the faster time scales these ionization losses are negligible in the hydrogen calculations.

The effect of collisional ionization and excitation on the electron temperature is better seen in Figures 7 and 8. They show the electron and ion temperatures on the axis of the plasma cylinder as a function of time for 10 mtorr H_2 and argon. In order to be able to discard of energy losses caused by heat conduction calculations with a superposed magnetic field are shown (c.f. Table 1). The solid curves are for the same conditions that were used for the calculations of Figures 1 to 6, i.e. taking into account ionizing collisions but disregarding excitational collisions ($S \neq 0, P = 0$). The dashed curves represent calculations in which collisions with the neutral background were neglected entirely ($S = 0, P = 0$), whereas for the dash-dotted curves of Figure 7 both ionization and excitation were taken into account ($S \neq 0, P \neq 0$). How strong the electrons are cooled by collisions with the neutral background depends, of course, on the degree of ionization α and on the electron temperature. In the hydrogen calculations ionization losses are negligible even for a relatively small degree of ionization of 3 %, whereas for the argon calculations ionizing collisions reduce the equilibration temperature by about 10 % for $\alpha \approx 15$ % and by about 20 % for $\alpha \approx 3$ %. Energy losses due to excitational collisions are more severe, as indicated for hydrogen in Figure 7. For the cross-sections used they reduce the equilibration temperature by about 10 % for $\alpha \approx 15$ %, but by about 30 % for $\alpha \approx 3$ %.

Garching

W. Lotz, Z. Physik 216, 39 (1968)

A.W. All and A.D. Anderson, Report NAL 207, Naval Research Laboratory, Washington, D.C. (1969)

IV. Conclusions

The numerical calculations allow us to draw the following conclusions on the time evolution of plasma preionized by ultraviolet radiation.

- 1) The time for energy equipartition between electrons at 2 eV and ions at 0.1 eV is a few μsec for H^+ and of order 100 μsec for Ar^+ . By waiting an appropriate time after firing the light source values of T_e/T_i ranging from 1 to about 10 can be selected in the photoionized plasma. This is an interesting feature of this preionization method, especially for its application to collision-free shock studies.
- 2) In a tube of 20 cm radius the decay of density is small during times of the order of the energy equipartition time. The same is true of energy losses due to radial heat conduction if an axial magnetic field of the order of 100 gauss is superimposed.
- 3) The amount of cooling of the electrons due to collisions with the neutral gas background (ionization and excitation) during their energy equipartitioning with the ions depends, of course, on the degree of ionization produced by the UV radiation and on the initial temperature of the electrons. If the degree of ionization is 10 to 20 % or more, as is the case in the discussed preionization experiment, then the electrons heat the ions faster than they lose energy to the neutral gas background. Starting with 2 eV electrons and 0.1 eV H^+ ions, energy losses caused by collisions with the neutral gas reduce the equilibration temperature by about 10 %.

I am grateful to Dr. R. Gorenflo and Mr. J. Steuerwald for developing the necessary computer program and for carrying out the numerical calculations.

Literature

- /1/ G.Hofmann, J.Quant.Spectr.Rad.Transfer 8, 729 (1968)
- /2/ F.Pecorella and G.Vlases, Phys.Lett. 28A, 616 (1969)
- /3/ F.Pecorella, G.C.Vlases, and M.Keilhacker, Bull.Am.Phys.Soc. 13, 1560 (1968)
- /4/ M.Keilhacker, F.Pecorella and G.Vlases, Report IPP 1/99, Institut für Plasmaphysik, Garching bei München (1969)
- /5/ M.Keilhacker, F.Pecorella, and G.Vlases, Phys. Fluids (in press)
- /6/ R.Chodura, M.Keilhacker, M.Kornherr, and H.Niedermeyer, Plasma Physics and Controlled Nuclear Fusion Research, Vol.I, 81, International Atomic Energy Agency, Vienna (1969)
- /7/ M.Keilhacker, M.Kornherr, and H.Niedermeyer (to be published)
- /8/ S.C.Brown, Introduction to Electrical Discharges in Gases, p. 71, J.Wiley and Sons, New York (1966)
- /9/ D.Düchs, Report IPP 1/14, Institut für Plasmaphysik, Garching bei München (1963)
- /10/ Reference /8/, p. 10
- /11/ L.Spitzer, Physics of Fully Ionized Gases, 2nd ed., p.133-135, J.Wiley and Sons, New York (1965)
- /12/ G.Herppich, Report IPP 4/68, Institut für Plasmaphysik, Garching bei München (1969)
- /13/ D.R.Bates, A.E.Kingston, and R.W.P.Mc Whirter, Proc.Roy.Soc. A 267, 297 (1962)
- /14/ W.Lotz, Z.Physik 216, 241 (1968)
- /15/ A.W.Ali and A.D.Anderson, Report NRL 6789, Naval Research Laboratory, Washington, D.C. (1969)

Table 1

Initial values for numerical results of Figures 1 - 8

Figure	1a	1b	2a	2b	3a	3b	4a	4b	5a	5b	6a	6b
				7a		7b				8a		8b
Gas			Hydrogen			Argon						
R (cm)	20		20		20		20		20		20	
p (mtorr)	1		10		10		1		10		10	
$n_e(0) \times 10^{-13} \text{ (cm}^{-3}\text{)}$	1		1		5		1		1		5	
α (%)	30		3		15		30		3		15	
$T_e(0)$ (eV)	2		2		2		2		2		2	
$T_i(0)$ (eV)	.1		.1		.1		.1		.1		.1	
B_0 (gauss)	0	50	0	50	0	200	0	200	0	200	0	200

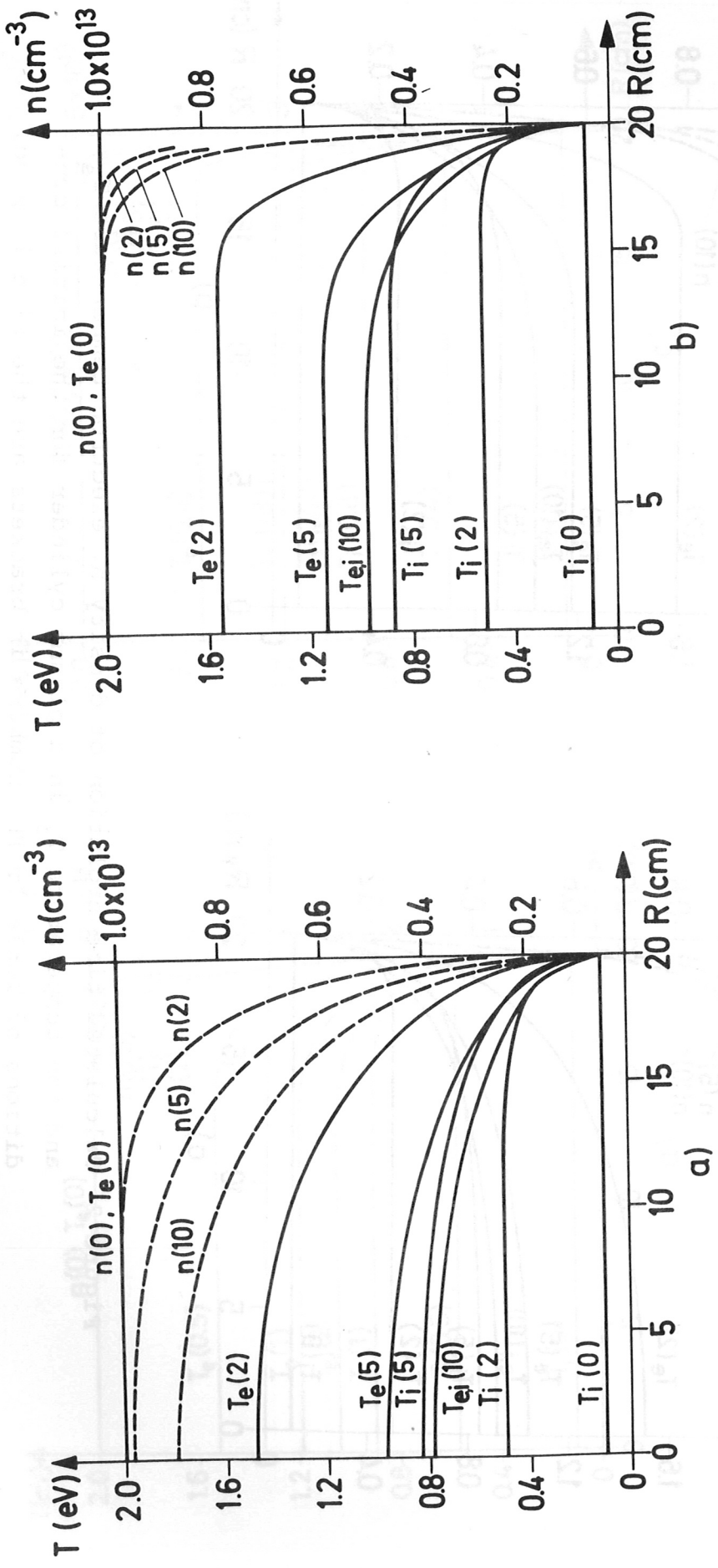


Figure 1 Calculated time evolution of density n , electron temperature T_e , and ion temperature T_i in a plasma cylinder for the initial conditions of Table 1. The numbers in brackets are the time in μsec . 1 mtorr H_2 , $\alpha = 30\%$, a) $B_0 = 0$ b) $B_0 = 50$ gauss

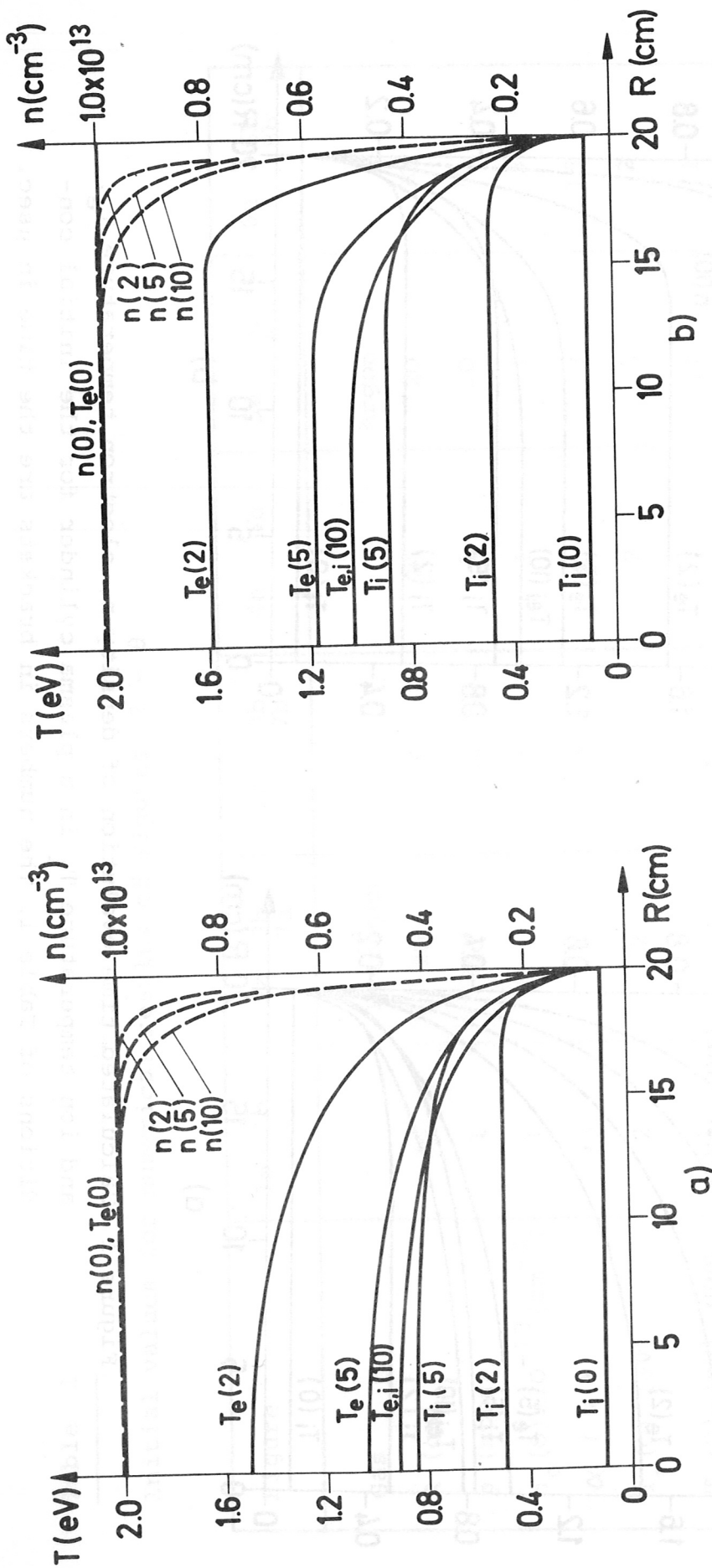


Figure 2 Calculated time evolution of density n , electron temperature T_e , and ion temperature T_i in a plasma cylinder for the initial conditions of Table 1. The numbers in brackets are the time in μsec . 10 mtorr H_2 , $\alpha = 3\%$, a) $B_0 = 0$ b) $B_0 = 50$ gauss

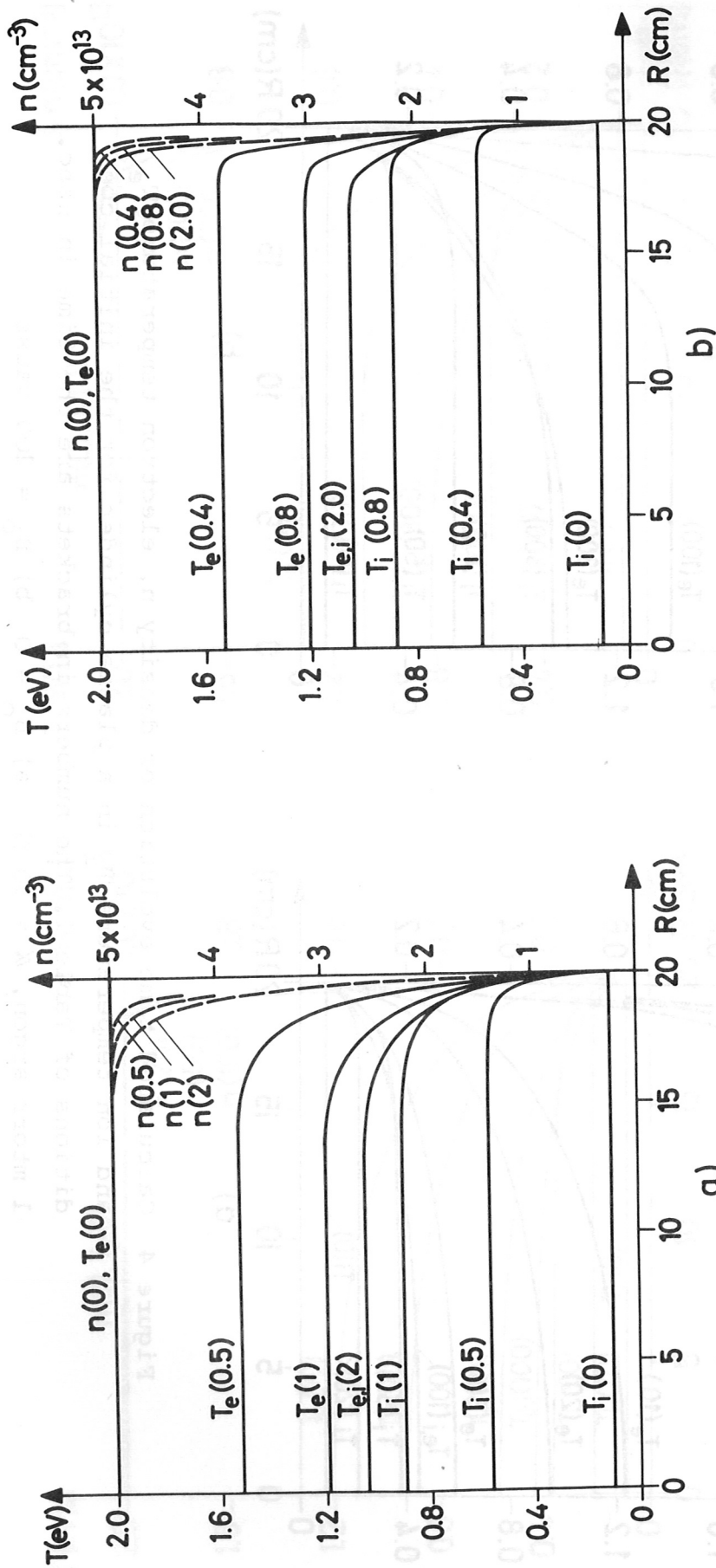


Figure 3 Calculated time evolution of density n , electron temperature T_e , and ion temperature T_i in a plasma cylinder for the initial conditions of Table 1. The numbers in brackets are the time in μsec . 10 mtorr H_2 , $\alpha = 30\%$, a) $B_0 = 0$ b) $B_0 = 200$ gauss

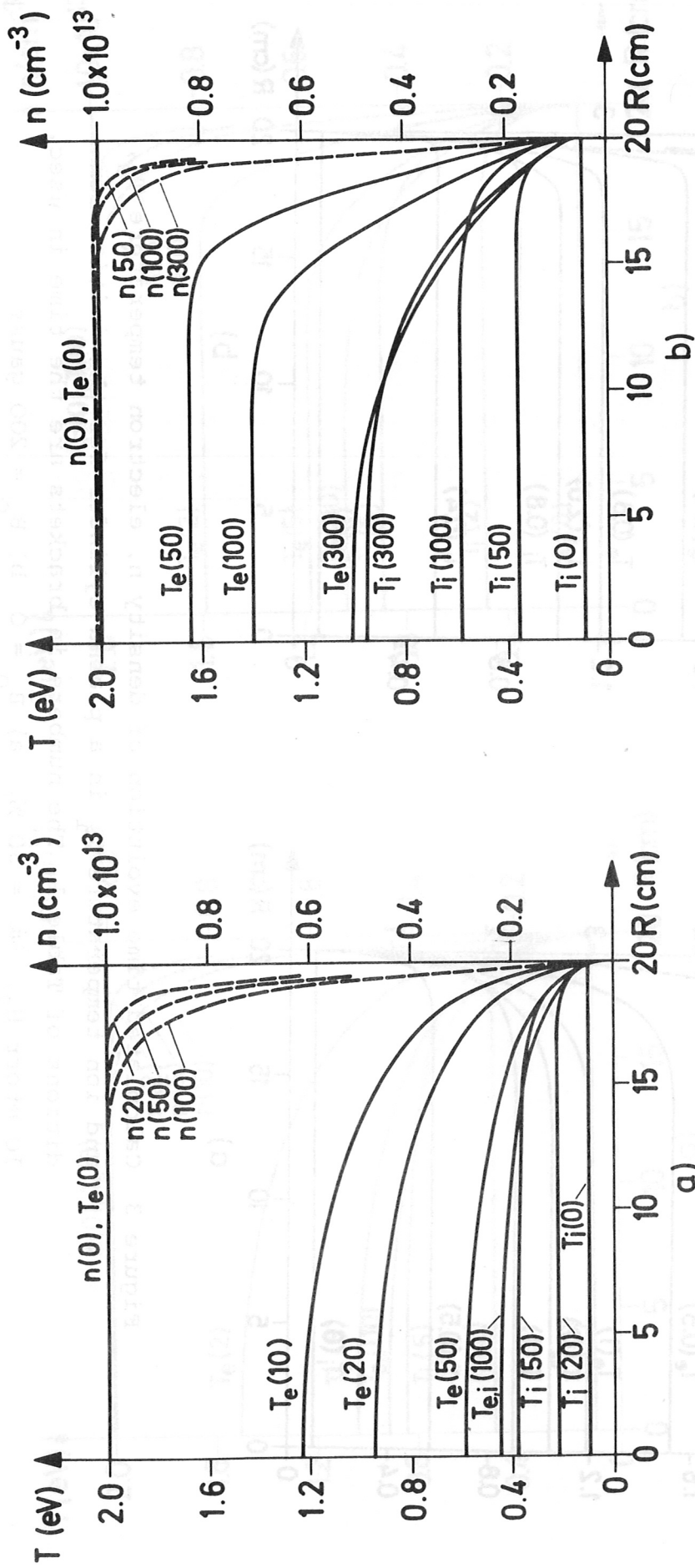


Figure 4 Calculated time evolution of density n , electron temperature T_e , and ion temperature T_i in a plasma cylinder for the initial conditions of Table 1. The numbers in brackets are the time in μsec . 1 mtorr argon, $\mathcal{N} = 30\%$, a) $B_0 = 0$ b) $B_0 = 200$ gauss

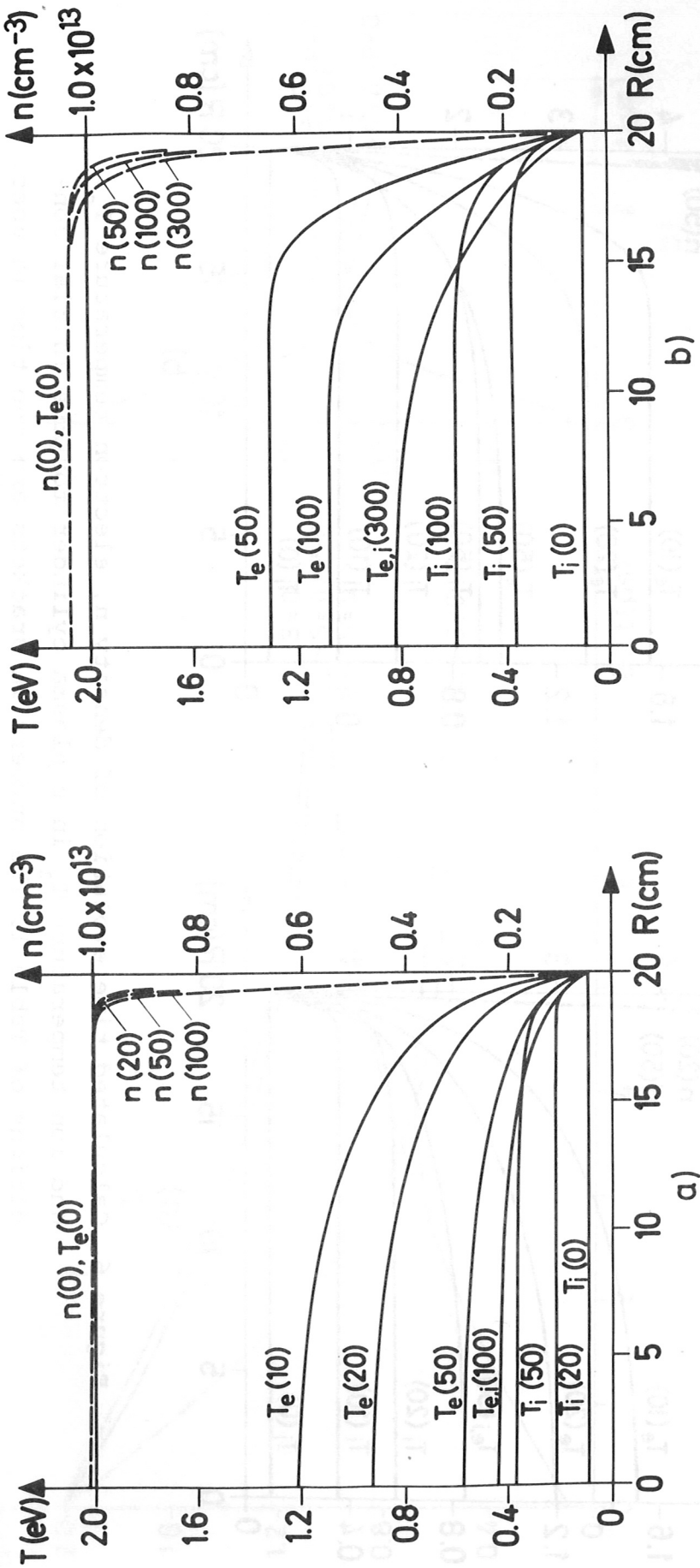


Figure 5 Calculated time evolution of density n , electron temperature T_e , and ion temperature T_i in a plasma cylinder for the initial conditions of Table 1. The numbers in brackets are the time in μsec . 10 mtorr argon, $\alpha = 3\%$, a) $B_0 = 0$ b) $B_0 = 200$ gauss

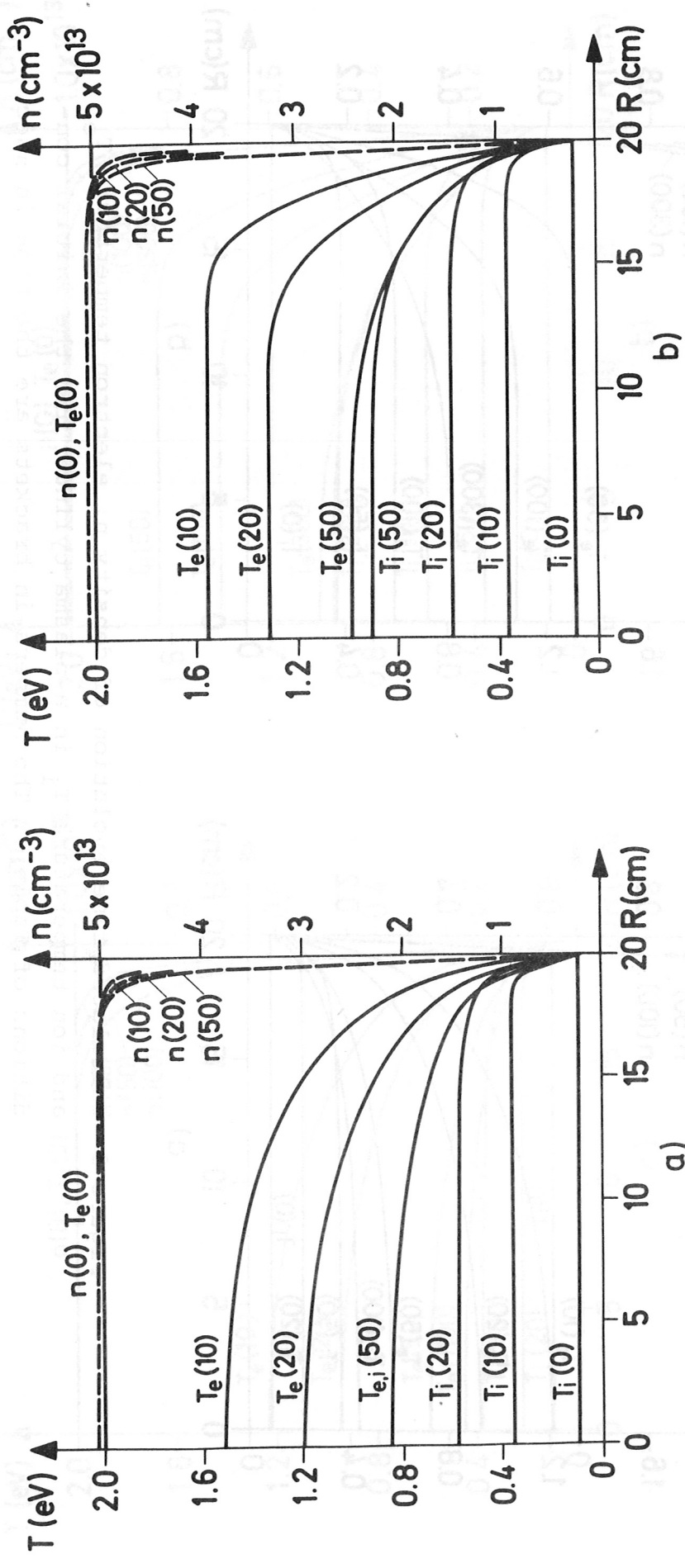


Figure 6 Calculated time evolution of density n , electron temperature T_e , and ion temperature T_i in a plasma cylinder for the initial conditions of Table 1. The numbers in Brackets are the time in μsec . 10 mtorr argon, $\alpha = 15\%$, a) $B_0 = 0$ b) $B_0 = 200$ gauss

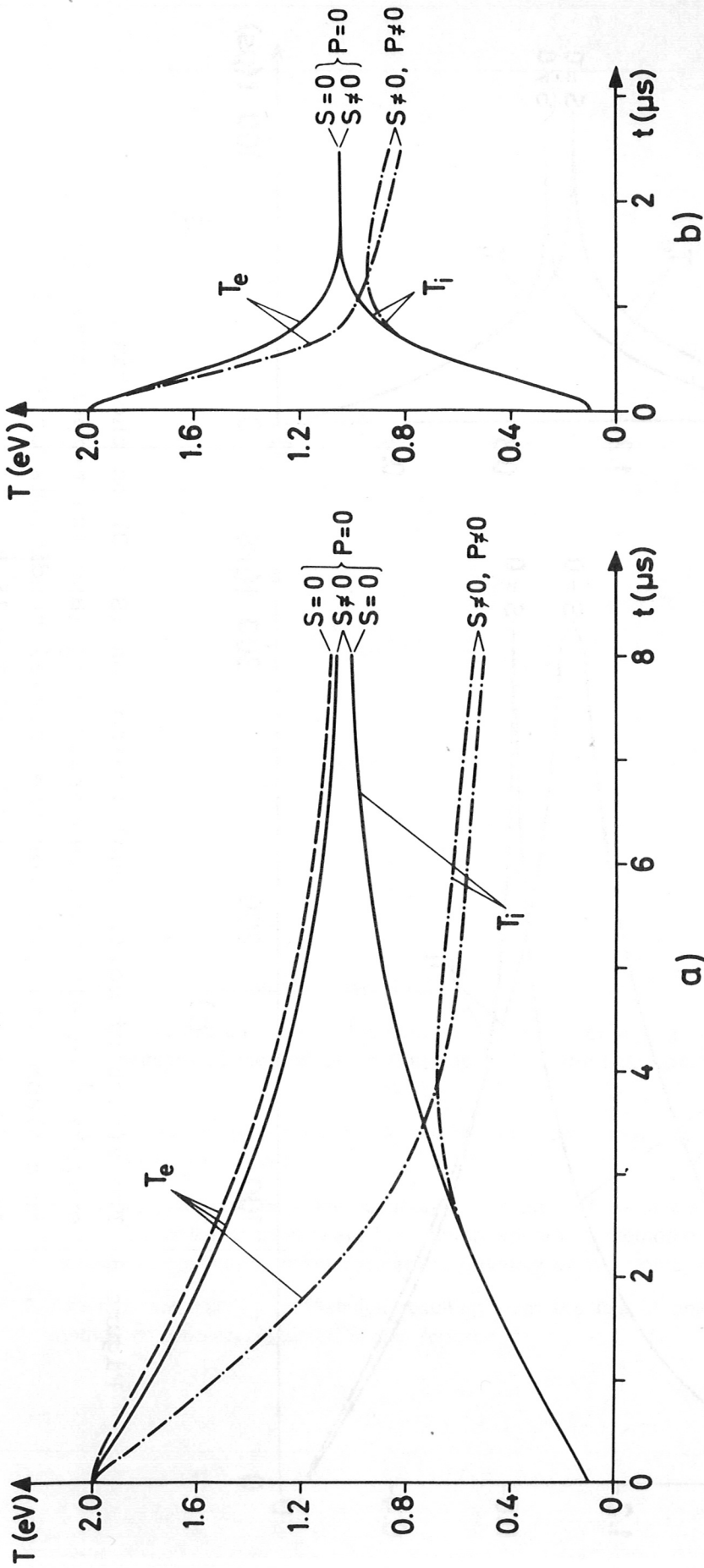


Figure 7 The effect of collisional ionization ($S \neq 0$) and excitation ($P \neq 0$) on the time evolution of electron temperature T_e (and ion temperature T_i) in a plasma cylinder for the initial conditions of Table 1. 10 mtorr H_2 a) $\chi = 3\%$ b) $\chi = 15\%$.

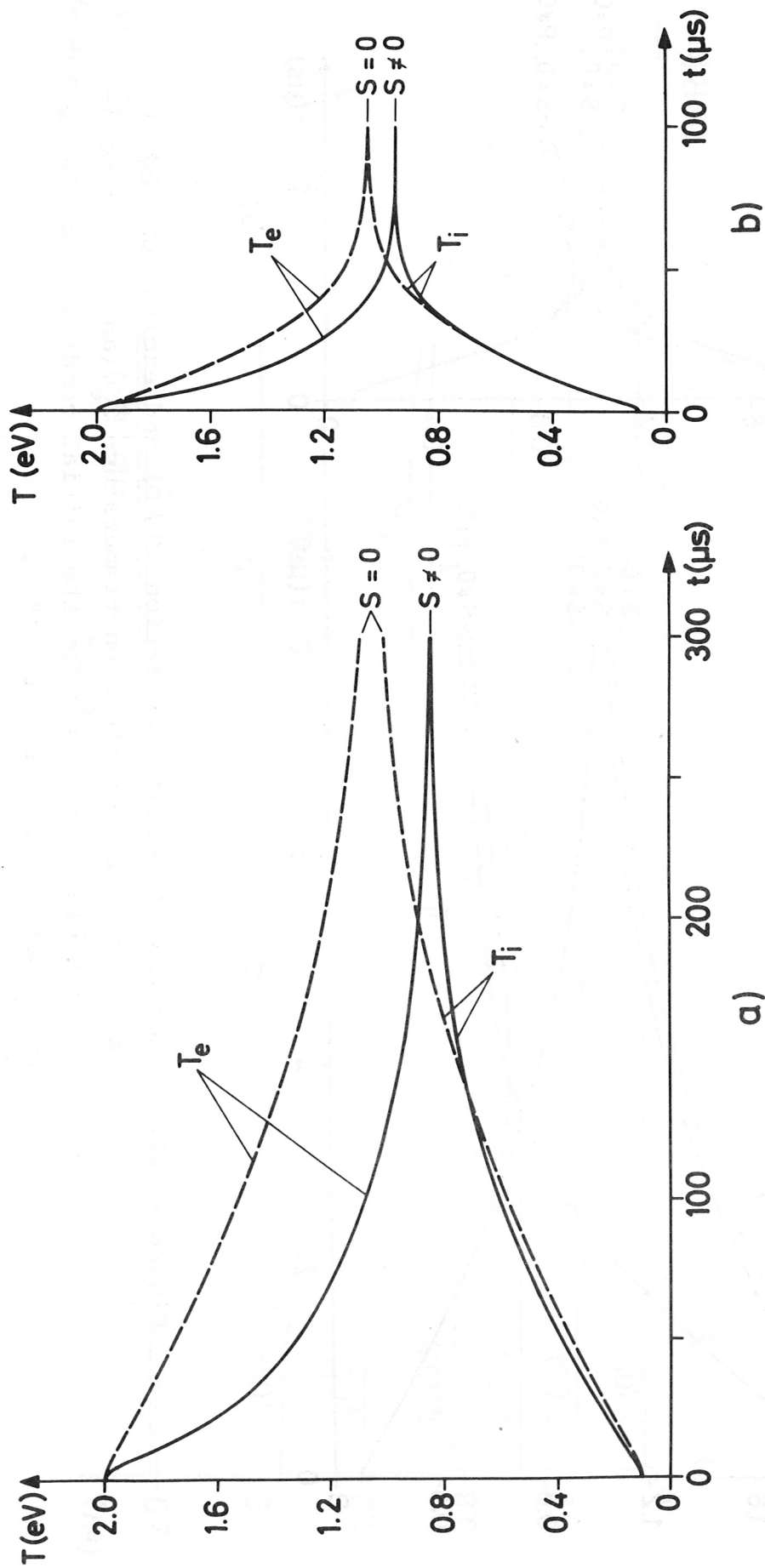


Figure 8 The effect of collisional ionization ($S \neq 0$) on the time evolution of electron temperature T_e (and ion temperature T_i) in a plasma cylinder for the initial conditions of Table 1. 10 mtorr argon a) $\alpha = 3\%$ b) $\alpha = 15\%$.